

Oxygen Induced Reconstruction of the Rh(100) Surface: General Tendency Towards Threefold Oxygen Adsorption Site on Rh Surfaces

A. Baraldi,¹ J. Cerdá,² J. A. Martín-Gago,² G. Comelli,^{1,3,4} S. Lizzit,¹ G. Paolucci,¹ and R. Rosei^{3,4}

¹*Sincrotrone Trieste S.C.p.A., S.S. 14 Km 163.5, 34012 Trieste, Italy*

²*Instituto de Ciencia de Materiales de Madrid, CSIC, Cantoblanco, 28049 Madrid, Spain*

³*Dipartimento di Fisica, Università di Trieste, 34127 Trieste, Italy*

⁴*Laboratorio T.A.S.C.-I.N.F.M., Padriciano 99, 34012 Trieste, Italy*

(Received 28 December 1998)

On the basis of a low energy electron diffraction I - V structural investigation, the surface geometry of the Rh(100) + (2 × 2)-2O phase has been determined. The oxygen is found to adsorb in an unusual threefold site of the rhombi created by the reconstruction of the first rhodium layer, producing a pg symmetry, in agreement with theoretical predictions but at variance with previous experimental conclusions. Our result indicates that there is a strong tendency of oxygen to adsorb in threefold sites on all Rh surfaces. [S0031-9007(99)09340-0]

PACS numbers: 68.35.Bs, 61.14.Hg

The adsorption geometry of atoms on single crystal surfaces is closely related to many of the fundamental properties of a surface overlayer: determination of the adsorption site, bond length, and site symmetry contribute in a fundamental way to the understanding of electronic and vibrational surface properties. In this context, low energy electron diffraction (LEED) [1] has proven to be one of the most powerful techniques, since a qualitative inspection of the diffraction pattern already provides important information on the periodicity and symmetry of the system under investigation, while a theory-experiment comparison of the LEED I - V curves permits the determination of the atomic positions. Among the symmetry properties that a surface may exhibit [2], the existence of glide planes represents a special case, since at normal LEED incidence it leads to the systematic absence of some diffraction spots and, can, therefore, be easily detected experimentally.

One example is the nonprimitive (2 × 2) oxygen structure obtained on Rh(100) at 0.5 ML. This structure has been previously investigated using LEED [3–8], scanning tunneling microscopy (STM) [8], core level photoemission [9], angle resolved photoemission [10], and angle resolved ion scattering (ARIS) [11]. At normal incidence, the LEED $(n + 1/2, 0)$ and $(0, m + 1/2)$ spots for this system were absent and since, in principle, this may result either from a $p4g$ or a pgg symmetry, the actual space group symmetry of this surface had been a subject of debate.

STM results clearly showed a fourfold-type reconstruction of the top rhodium layer, which appeared to confirm the $p4g$ symmetry [8]. From the comparison of these STM images with those of the closely related C and N on Ni(100) systems [12], for which a quantitative structural determination has been performed, a structural model was proposed, where the oxygen atoms occupy hollow sites of the first Rh layer, with alternative clockwise and counterclockwise rotations of the occupied Rh squares. More recently an ARIS investigation con-

firmed this model [11], which we indicate as “B” (black) reconstruction [Fig. 1(a)].

However, very recent *ab initio* theoretical calculations carried out for this system by Alfè *et al.* [13] concluded that the reconstruction consists of the same type of rotations but applied to the empty Rh squares, i.e., rotations around the empty hollow sites. We show this model, indicated as “W” (white) reconstruction, in Fig. 1(b). Although both models present a $p4g$ symmetry, their oxygen bonding geometries differ considerably. In B, the oxygen atoms essentially maintain the fourfold arrangement of the $c(2 \times 2)$ geometry (adsorption at the hollow site), whereas in model W the local symmetry is reduced and the adsorbate is now located at the centers of the rhombi, so that for large enough Rh in-plane displacements, the adsorption site may be regarded as pseudobridge. Moreover, the model W predicted by Alfè *et al.* presents an even lower minimum in energy, when the oxygen atoms move from the pseudobridge site along the main diagonal of the rhombus, becoming essentially threefold coordinated. The group symmetry for this new model is though reduced from $p4g$ to pg , and therefore the $(n + 1/2, 0)$

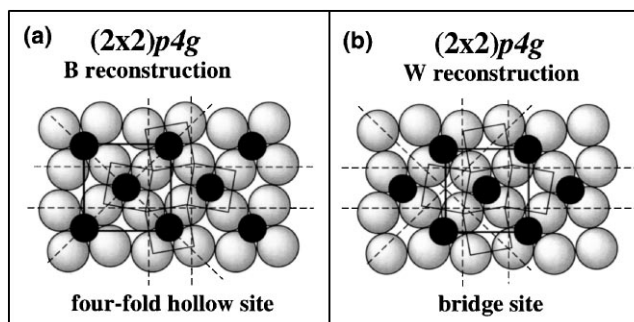


FIG. 1. Top views of the black “B” (a) and white “W” (b) models for the Rh(100) (2 × 2) $p4g$ -2O phase. Surface unit cells (thick lines), top Rh layer reconstruction (thin lines), and glide symmetry lines (dashed lines) are shown.

and $(0, m + 1/2)$ spots in the LEED pattern should not be missing, in contrast to what was experimentally observed.

In order to clarify this still open problem, we report in this Letter the results of our LEED I - V experiment on the Rh(100) + (2×2) -2O system.

The experiment was performed in the ultrahigh vacuum chamber of the SuperESCA beam line of ELETTRA, which is equipped with a Fisons rearview LEED instrument. The Rh(100) sample was prepared by a sputter-annealing-oxidation procedure as previously reported [4–7]. The (2×2) -2O structure has been prepared by oxygen exposure of 20 L (1 L = 10^{-6} mbar s) at 370 K. The LEED I - V curves, collected at 150 K by using a CCD camera, are shown in Fig. 2 as solid lines.

On the theoretical part, we have performed full-dynamical LEED I - V curves calculations with modified versions of the Tong-Huang codes [1,14–17]. These programs include symmetrization both in real and reciprocal space so that, for relatively simple systems (small and/or highly symmetric surface unit cells), I - V curves for thousands of trial structures may be calculated at a moderate computational cost.

In the calculations, we simulated the surface by stacking the oxygen overlayer and the two first Rh layers on top of a Rh bulk with a lattice parameter of $a = 1.902$ Å. We employed up to a total of 277 beams and 8 phase shifts per element which were computed relativistically with the Van Hove–Barbieri package and were then spin aver-

aged [19]. Nonstructural parameters such as the muffin-tin radii of the elements, the imaginary part of the energy, E_i , or the Debye temperatures, Θ_D , were checked during the optimization processes and corrected accordingly.

We employed Pendry's reliability factor, R_p , in order to quantify the theory-experiment I - V curves agreement [18], while error bars were estimated from the R_p variance, ΔR_p , which is given by [18]: $\Delta R_p = R_p^{\min} = \sqrt{\{8E_i/\Delta E\}}$, where ΔE corresponds to the total energy range analyzed (in our case, 2312 eV).

The structural analysis for the Rh(100) (2×2) -2O system has been carried out in several stages. In the first step, in order to discriminate between the B and W reconstructions, we have performed R_p optimizations for both cases by considering a multidimensional grid in the hyperspace of structural parameters. Only trial structures preserving a $p4g$ symmetry were considered (see Fig. 1), which leaves the oxygen overlayer unchanged from the $c(2 \times 2)$ phase. We also ignored any buckling of the second Rh layer, so that we varied a total of four structural parameters, namely, the first three interlayer spacings and the in-plane displacement of the first layer Rh atoms, δ_{Rh} . The resulting R_p optimization clearly favors model W ($R_p = 0.35$) over model B ($R_p = 0.44$). Since the R_p variance around the latter is $\Delta R_p(W) = 0.05$, model B can be safely ruled out, in accordance with the theoretical predictions. Further evidence is given by comparing the R_p behavior for each model as a function of δ_{Rh} , as shown in Fig. 3(a). R_p shows a clear minimum at $\delta_{Rh} = 0.20$ Å for model W, whereas for model B, R_p continuously increases as δ_{Rh} is increased.

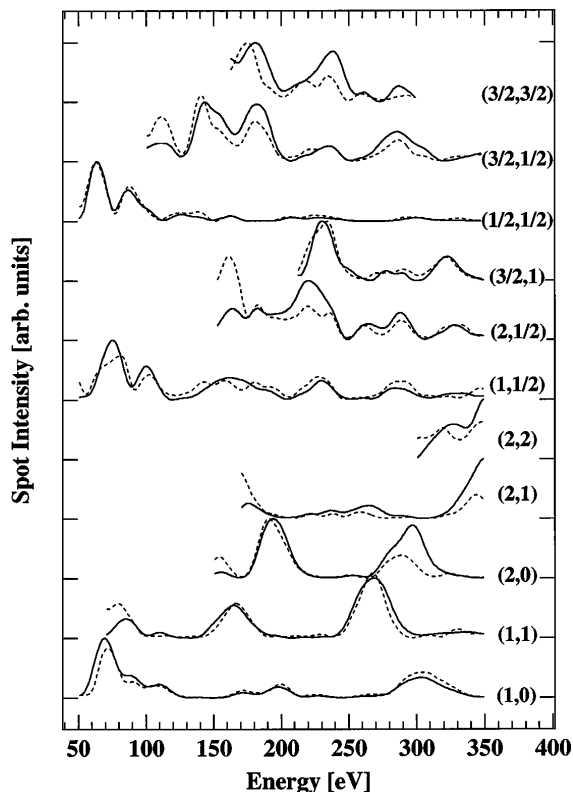


FIG. 2. Experimental (solid lines) and theoretical (dashed lines) LEED I - V curves for the Rh(100) (2×2) pg -2O system.

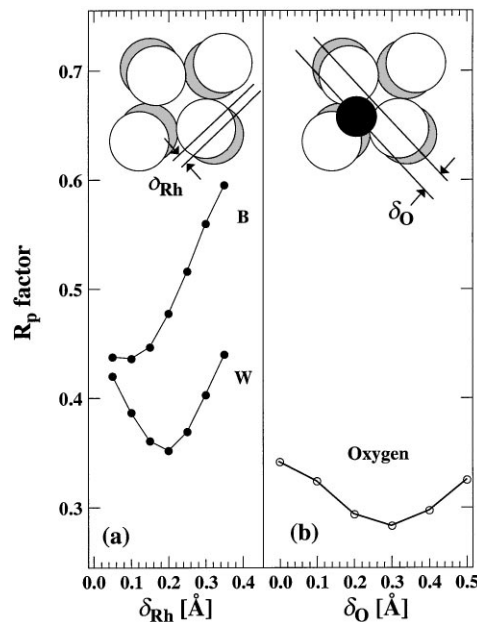


FIG. 3. R_p vs (a) in-plane displacement of the first layer Rh atoms, δ_{Rh} , for the models “B” and “W” and (b) in-plane displacement of the O atoms, δ_O . For each δ_{Rh} (δ_O) value in the graph, the R_p value corresponds to the minimum within the other parameters hyperspace.

Further refinements for this model, this time allowing for buckling of the second Rh layer, hardly improved the fit ($R_p = 0.34$), while the optimized coordinates were almost unchanged. The final geometry deduced in this way leads to two different oxygen-rhodium bond lengths: $d_{\text{O-Rh}} = 2.3 \text{ \AA}$, and $d_{\text{O-Rh}} = 2.0 \text{ \AA}$. While the shortest distance is close to the bond length found for the $p(2 \times 2)\text{-O}$ phase, the larger one is about 10% expanded. Interestingly, the second Rh layer presents no buckling and, therefore, hardly contributes to the (2×2) reconstruction.

Although the overall agreement is acceptable, a value of $R_p = 0.34$ is still somewhat large, suggesting that the substrate reconstruction, by itself, cannot fully explain the structural transition from the $c(2 \times 2)$ phase to the (2×2) . Hence, we also considered the possibility of distortions in the $c(2 \times 2)$ oxygen overlayer. As already mentioned, the theoretical calculations of Alfè *et al.* predicted that the oxygen atoms move away from the pseudobridge sites towards one of the Rh atoms located at the corners of the rhombi, adopting a local threefold adsorption geometry. Obviously, there are four symmetry-equivalent configurations depending on towards which of the centers of the two adjacent triangles the two oxygen atoms shift.

This asymmetric model is shown in Fig. 4. The distortion of the $c(2 \times 2)$ oxygen overlayer drastically reduces the symmetry of the system from a $p4g$ to a pg : both oxygen atoms are still symmetry equivalent, while in the first and second Rh layers there are two different inequivalent atoms, so that, in principle, the surface structure comprises now up to a total of 15 parameters. However, since rhodium is a strong scatterer as compared to oxygen, any small distortion of the $p4g$ symmetry at the first Rh layer already yields non-negligible intensities for the $(0, m + 1/2)$ and $(n + 1/2, 0)$ spots, which is in contrast with the experimental evidence. Therefore, in the searches for this asymmetric model we have only considered, besides all the parameters optimized in the previous step, the in-plane displacements of the oxygen atoms along the main diagonal of the rhombi,

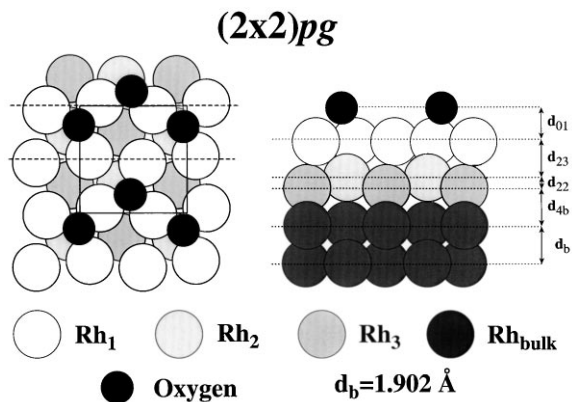


FIG. 4. Top and side views of the Rh(100) $(2 \times 2)pg\text{-}2\text{O}$ structure. Unit cell and glide lines are indicated in the top view (left).

δ_{O} (i.e., we imposed a local $p4g$ symmetry to the first two Rh layers). In order to recover the experimental diffraction pattern symmetry, we added the theoretical LEED intensities arising from the four symmetry related domains through a proper beam intensity averaging. This procedure is equivalent to regard the two oxygen atoms as incoherently hopping between their adjacent triangles, which is precisely the situation proposed by Alfè *et al.*

We plot in Fig. 3(b) the R_p vs δ_{O} behavior obtained from these searches. Once again, the R_p analysis confirmed the theoretical predictions, since a new minimum was found, $R_p = 0.28$, for an oxygen displacement of $\delta_{\text{O}} = 0.3 \text{ \AA}$, while the R_p variance clearly excludes the symmetric model. Again, further refinements hardly introduced any improvements to the fit. The final optimized parameter values, corresponding to $R_p = 0.28$, are $d_{01} = 1.05 \pm 0.05 \text{ \AA}$, $d_{12} = 1.94 \pm 0.02 \text{ \AA}$, $d_{22} = 0.00 \pm 0.03 \text{ \AA}$, $d_{23} = 1.87 \pm 0.03 \text{ \AA}$, $\delta_{\text{O}} = 0.29 \pm 0.15 \text{ \AA}$, and $\delta_{\text{Rh}} = 0.20 \pm 0.07 \text{ \AA}$. The theoretical LEED $I\text{-}V$ curves obtained from this set of parameters are shown as dashed lines in Fig. 2. The magnitude of the O displacements basically leaves the adsorbate atoms threefold coordinated: $d_{\text{O-Rh}} = 2.02 \text{ \AA}$ for the two Rh atoms forming the pseudobridge, while $d_{\text{O-Rh}} = 2.09 \text{ \AA}$ for the Rh at the corner of the rhombus. Apart from the considerable in-plane substrate reconstruction ($\delta_{\text{Rh}} = 0.2 \text{ \AA}$), we also find a slight 2% expansion (contraction) between the first and the second (second and third) Rh layers with respect to the bulk interlayer distance $d_b = 1.902 \text{ \AA}$. This is a typical behavior for metal surfaces with highly electronegative species adsorbed, and stems from the metal charge transfer to the adsorbate.

It is important to notice that, despite the large δ_{O} value, since the oxygen scattering strength is weak, the expected domain-averaged intensity for the $(n + 1/2, 0)$ and $(0, m + 1/2)$ spots is, on the average, 1 order of magnitude smaller than the intensity for the rest of the half-order spots, and 2 orders of magnitude smaller with respect to the integer order beams. Such a low intensity can explain why these spots were regarded as absent in the previous experimental works and, consequently, the symmetry of this phase was erroneously assigned to the $p4g$ group. Indeed also in our experiment these spots could be distinguished from the background only after prolonged intensity integration and at specific electron kinetic energies [e.g., 74 eV for the $(1/2, 0)$ spot]. It is interesting to note that these energies are in good agreement with the intensity maxima predicted by our simulations.

Our model involves in-plane displacements for the O and Rh atoms which are in very good agreement with the values proposed by Alfè *et al.* [13]. On the basis of our data though we can rule out the 0.08 \AA buckling in the first Rh layer they found, as this would increase the intensity of the $(0, 1/2)$ and $(1, 1/2)$ beams by an order of magnitude, without improving the R_p .

On the other hand, our geometry is at contrast with the ARIS study, which proposed the B model with an unusually small O-Rh distance: $d_{O1} = 0.6 \pm 0.1 \text{ \AA}$ [11]. We have found a very large R_p value ($R_p = 0.71$) for this geometry, which therefore is not compatible with our data. However, it should be noted that the δ_{Rh} value deduced in Ref. [11] is in very close agreement with the value found in this work. It still needs to be explained why the STM images show a $c(2 \times 2)$ arrangement of the adsorbed oxygen atoms. As previously suggested [13], this could be related to the different temperature of the STM experiment, which could induce oxygen hopping between two inequivalent low-symmetry sites at a frequency higher than the STM scanning frequency.

Our result shows that there is a general tendency of oxygen to adsorb in threefold sites on Rh surfaces. In the present case, where such sites are not available, the adsorbate forces the substrate to reconstruct. The driving force for the reconstruction is therefore the energy gain determined by the optimization of the O-Rh bond [13]. This results in a very similar local environment for oxygen on Rh surfaces, i.e., similar bond lengths, bond angles, and symmetry, regardless of the symmetry of the substrate. In fact, on all low Miller index Rh surfaces, for medium-high oxygen coverages the O-Rh bond length is in the 2.00–2.06 Å range, the symmetry threefold, and the Rh-O-Rh angle around 90° [20].

This observed peculiarity of Rh towards dissociative oxygen adsorption with respect to the other transition metal surfaces could be a key point for the understanding of the unique properties of rhodium as NO reduction catalyst. In fact, it has recently been suggested that the energy of the transition state for a simple dissociation reaction closely follows the energy of the reaction final state, i.e., the adsorption energy of the chemisorbed atoms alone [21], which is strictly related to the local geometry around the reaction products. The possibility for atomic oxygen to attain an ideal threefold geometry on all low Miller index Rh surfaces could explain the very high activity of this metal towards NO dissociation.

In conclusion, our work settles the controversy regarding the (2×2) -2O surface structure on Rh(100), indicating that the preferred adsorption site for oxygen is a rather unusual threefold site, in good agreement with a previous theoretical calculation. Moreover, we show that the reconstructed surface, induced by the oxygen adsorption, presents a pg surface symmetry which was not previously identified by simple inspection of the diffraction pattern, due to the very low intensity of some of the diffraction spots. A general tendency for oxygen to adopt the same local environment on different Rh surfaces is highlighted.

Discussions with D. Alfè, S. Baroni, S. de Gironcoli, K.C. Prince, and M. Kiskinova are gratefully acknowledged. J.C. acknowledges financial support from

the Spanish Ministerio de Educacion y Ciencia and from the Spanish CICYT under Contract No. PB94-1530 and No. PB96-0916. G.C. and R.R. acknowledge financial support from the MURST under the program "COFIN97."

-
- [1] M.A. Van Hove and S.Y. Tong, *Surface Crystallography by LEED* (Springer-Verlag, Berlin, 1979).
 - [2] D.P. Woodruff and T.A. Delchar, *Modern Techniques of Surface Science*, Cambridge Solid State Science Series (Cambridge University Press, Cambridge, England, 1986).
 - [3] W. Oed, B. Dötsch, L. Hammer, K. Heinz, and K. Müller, *Surf. Sci.* **207**, 55 (1988).
 - [4] L. Gregoratti, A. Baraldi, G. Comelli, V.R. Dhanak, M. Kiskinova, and R. Rosei, *Surf. Sci.* **340**, 205 (1995).
 - [5] A. Baraldi, L. Gregoratti, G. Comelli, V.R. Dhanak, M. Kiskinova, and R. Rosei, *Appl. Surf. Sci.* **99**, 1 (1996).
 - [6] A. Baraldi, V.R. Dhanak, G. Comelli, K.C. Prince, and R. Rosei, *Phys. Rev. B* **53**, 4073 (1996).
 - [7] A. Baraldi, V.R. Dhanak, G. Comelli, K.C. Prince, and R. Rosei, *Phys. Rev. B* **56**, 10511 (1997).
 - [8] J.R. Mercer, P. Finetti, F.M. Leibsle, R. McGrath, V.R. Dhanak, A. Baraldi, K.C. Prince, and R. Rosei, *Surf. Sci.* **352**, 173 (1996).
 - [9] M. Zacchigna, C. Astaldi, K.C. Prince, M. Sastry, C. Comicioli, R. Rosei, C. Quaresima, C. Ottaviani, C. Crotti, A. Antonini, M. Matteucci, and P. Perfetti, *Surf. Sci.* **347**, 53 (1996).
 - [10] J.R. Mercer, P. Finetti, M.J. Scantlebury, U. Beierlein, V.R. Dhanak, and R. McGrath, *Phys. Rev. B* **55**, 10014 (1997).
 - [11] Y.G. Shen, A. Qayyum, D.J. O'Connor, and B.V. King, *Phys. Rev. B* **58**, 10025 (1998).
 - [12] L. Wenzel *et al.*, *Phys. Rev. B* **36**, 7689 (1987); M. Bader *et al.*, *Phys. Rev. B* **35**, 5900 (1987); T.S. Rahman and H. Ibach, *Phys. Rev. Lett.* **54**, 1933 (1985); C.F. McConville *et al.*, *Phys. Rev. B* **34**, 2199 (1986); G. Hörmandinger *et al.*, *Phys. Rev. B* **48**, 8356 (1993); A.L.D. Kilcoyne *et al.*, *Surf. Sci.* **253**, 107 (1991); F.M. Leibsle *et al.*, *Surf. Sci.* **297**, 98 (1993).
 - [13] D. Alfè, S. de Gironcoli, and S. Baroni, *Surf. Sci.* **410**, 151 (1998).
 - [14] W.H. Press *et al.*, *Numerical Recipes: The Art of Scientific Computing* (Cambridge University Press, Cambridge, England, 1989).
 - [15] J. Cerdà, F.J. Palomares, and F. Soria, *Phys. Rev. Lett.* **75**, 665 (1995).
 - [16] J. Cerdà, Ph.D. thesis, Universidad Autonoma de Madrid, 1995.
 - [17] H. Huang *et al.*, *Phys. Lett. A* **130**, 166 (1988).
 - [18] J.B. Pendry, *J. Phys. C* **13**, 937 (1980).
 - [19] M.A. Van Hove and A. Barbieri (private communication).
 - [20] J.D. Batteas *et al.*, *Surf. Sci.* **339**, 142 (1995); M. Gierer *et al.*, *Surf. Sci.* **297**, L73 (1993); C. Comicioli *et al.*, *Chem. Phys. Lett.* **214**, 438 (1993); S. Schwegmann *et al.*, *Surf. Sci.* **375**, 91 (1997).
 - [21] J.K. Norskov *et al.*, *Abstr. Pap. Amer. Chem. Soc.* **215**, 68 (1998).